

negative impacts caused by this plant, governments and agencies allocate a significant amount of resources every year to control its invasion. Therefore, water hyacinth from an environmental perspective helps reduce weed growth, promote clean energy, and maintain aquatic ecosystems [9], [10]. Furthermore, water hyacinth has the potential to serve as a viable substitute for natural fibers in a variety of engineering applications, such as automotive components, when used as a composite reinforcement material. The high cellulose and hemicellulose content of water hyacinth renders it an exceptional material for composite reinforcement. It contains nearly 20% cellulose, 48% hemicellulose, and 3.5% lignin [11]. Therefore, developing natural fibers as eco-friendly polymer composite materials from water hyacinth plants is an ideal solution for producing versatile materials, especially in the automotive industry, and contributes to achieving SDGs [12].

With population growth and increased vehicle usage comes congestion and the risk of collisions. Therefore, strong bumpers are required to protect the vehicle, absorb impact energy, and minimize damage to the vehicle body to improve passenger safety. Bumper design plays an important role in improving impact resistance and overall vehicle safety [13], [14], [15]. Car bumpers are usually made of steel, aluminum, rubber, fiber, or plastic. Bumpers made of fiber are less safe as they are easily damaged, whereas plastic has the disadvantages of reduced impact resistance and high production costs [16], [17]. Natural fiber composites have significantly improved their structural, mechanical, and tribological properties over the past two decades [18], [19]. Currently, numerous automobile bumpers are constructed from natural fiber composites. Despite substantial studies on natural fibers as reinforcement in composite materials, the majority of studies continue to concentrate on widely utilized fibers such as kenaf, ramie, and coconut coir. *Eichhornia crassipes* (water hyacinth), despite its abundance and promising mechanical properties, has received limited attention, particularly in automotive applications, especially for bumper components [20], [21]. Furthermore, the weave pattern in fiber-based composites plays a crucial role in determining their impact and bending strength. However, studies combining *Eichhornia crassipes* fibers with specific weaving patterns remain scarce, especially in the context of impact-absorbing vehicle structures. This gap underscores the need for systematic research into the mechanical properties of woven *Eichhornia crassipes* composites for environmentally friendly, lightweight, yet strong automotive applications.

This research focuses on polymer matrix composites combining water hyacinth fiber and epoxy, because epoxy has better strength, stiffness, and corrosion resistance than other polymers, with better yield strength than thermoplastics, and is resistant to alkalis, acids, moisture, and high temperatures [22], [23]. However, most polymer composites with natural fibers have the disadvantage of being hydrophilic, leading to a weak interaction between the reinforcement and the matrix [24]. To mitigate this issue, alkali treatment is an approach that enhances the stress transfer capability and interfacial contact [25]. The alkaline treatment of natural fibers enhances surface irregularity, thereby facilitating a more effective interaction with the polymer matrix [26], [27]. Without alkalization, the bonding of fibers and resin is imperfect due to the waxy coating on the fibers. However, parameters such as alkali concentration, temperature, and soaking time must be well-regulated to prevent fiber damage, as excessive soaking can decrease fiber strength due to excessive delignification [28]. The mechanical strength of composites depends on the bonding of fibers and matrix, as well as factors such as fiber orientation. In this case, the water hyacinth fibers were woven in a specific orientation. Matting ensures the fibers are more organized, evenly distributed, and reduces anisotropy in the composite sheet [29], [30]. Fiber webbing provides better composite strength than parallel fibers, mainly since the reinforcement occurs in two mutually perpendicular directions, increasing the overall strength of the composite [31], [32]. For use in automobile bumpers, this research developed a composite material comprising 60% water hyacinth fiber and 40% epoxy resin by volume. Therefore, it is important to find out how strong this combination is mechanically, so that the study can lead to a different material for car bumpers that is just as safe and does not cost as much.

2. METHODS AND MATERIALS

This methodology can be divided into three main processes, starting with the initial preparation, which involves setting up the essential elements needed to begin the composite fabrication. At this stage, the preparation of materials, fiber treatment, and fiber orientation are explained in detail. The second and last phase involves composite molding into samples and conducting mechanical testing to assess the composite's mechanical strength. The subsequent phases are elucidated below.

2.1 Material

2.1.1 Water Hyacinth (*Eichhornia Crassipes*)

The water hyacinth stems used in this study were obtained from Ambarawa, Semarang, Indonesia (Figure 1). The water hyacinth plants in Lake Ambarawa, which grow prolifically and nearly cover the lake's surface, have stems that are rich in fiber [33]. These fibers are of high quality due to their strength and elasticity, and they are biodegradable. Furthermore, the raw material is readily available, abundant, inexpensive, and non-toxic, making its use as a composite material a potential solution to address this invasive plant [34]. The water hyacinth fiber has a Young's modulus of 10.60 MPa, tensile strength of 540 MPa, breaking strain of 1.3 MPa, and a density of 1.23 to 1.45 g/cm³ (Table 1).



Figure 1. Water hyacinth

Table 1. The physical and mechanical characteristics of water hyacinth fiber [35]

Properties	Value
Young's modulus (MPa)	10.6
Tensile strength (MPa)	540
Breaking strain (MPa)	1.3
Density (g/cm ³)	1.23-1.45

2.1.2 Epoxy Resin

Epoxy resin and hardener were purchased from the Nusakimia Abadi store in North Jakarta, Indonesia (Figure 2). This matrix adhesive is used to bond woven water hyacinth fibers. The resin consists of a blend of resin and hardener in a 2:1 ratio. Epoxy resin can enhance toughness, resistance to corrosion, heat resistance, and dimensional stability, and it is also easy to repair and adjust [36]. The high tensile and compressive strength of epoxy resin renders it an optimal choice for structural adhesives, as it is capable of withstanding hefty loads and pressure and preventing deformation [37]. Its high bonding strength makes it widely used in construction, shipbuilding, automotive, and aerospace industries. Epoxy resin has a tensile strength of up to 85 MPa and an elongation of 5%, with a density between 1.11 and 1.23 g/cm³, as seen in Table 2.



Figure 2. Epoxy resin and hardener

Table 2. The physical and mechanical characteristics of epoxy resin [38]

Properties	Value
Elongation at break (%)	5
Heat distortion temperature (°C)	120
Tensile strength (MPa)	~ 85
Density (g/cm ³)	1.11 ~ 1.23
Compressive strength (MPa)	~ 11
Tensile elastic modulus (GPa)	~ 3.2
Flexural strength (MPa)	~ 130
Linear expansion coefficient (in 10 ⁻⁶ /°C)	60
Water absorption/24 h (%)	0.14
Rockwell hardness/6.35 mm, 100 kg	100
Shrinkage rate (%)	1 ~ 2

2.2 Alkali Treatment

Sodium hydroxide (NaOH) was purchased from Indrasari Chemical Store, Semarang, Indonesia (Figure 3). The NaOH used is in powder form, which must be dissolved in distilled water (also known as aquades) for the alkalization mixture. The stems of the water hyacinth are cleaned with a wire brush to get fibers, which measure 350 mm in length. Next, a 20% sodium hydroxide (NaOH) solution is used for fiber processing. This 20% concentration is made by dissolving 200 grams of NaOH in 1000 ml of distilled water. The water hyacinth fibers are soaked in the alkaline solution for 3 hours, fully submerging the entire fiber. The fibers are then washed with clean water to remove any remaining alkaline solution. The fibers are rinsed and then left to dry at room temperature for 24 hours. Following the alkalization process, a visible physical change in the fibers is the color change, where the initially light brown fibers before alkalization turn dark brown after alkalization (Figure 4). The previous study has established that the optimal alkaline process for natural fibers, specifically water hyacinth fibers, is using a 20% NaOH solution for 3 hours, which increases the load-bearing capacity by 13.33% compared to composites treated with a 10% NaOH solution [39], [40]. A 20% NaOH treatment on natural fibers produces a rougher surface, enhancing adhesion between the fibers and the matrix during composite production. Among the myriad parameters, concentration emerges as the paramount factor in augmenting the mechanical strength of the composite material [41].



Figure 3. NaOH



(a)



(b)

Figure 4. Water hyacinth fiber (a) before alkalization; (b) after alkalization

2.3 Orientation of Woven Fiber Composite

In composites with aligned fibers, optimal strength is achieved when the load is applied parallel to the fibers. Nevertheless, its strength markedly diminishes when the force is exerted perpendicular to the fiber orientation. Therefore, optimizing the composite constituents requires weaving the reinforcing fibers. The weaving process aims to arrange the fibers more regularly and evenly in their distribution, thereby preventing anisotropy in the composite sheets. Woven fibers can enhance the composite's strength because the bonds between the woven fibers are stronger than those in non-woven fibers [42]. The weaving pattern involves various types of warp and weft orientations, which can be either homogeneous or hybrid. This study selected plain, twill, and basket weave patterns as variations for composite fiber orientation. The weaving process was conducted manually, without the use of a weaving machine. It begins with preparing twisted fibers, each measuring 300 mm in length. A frame or base is then constructed to hold the fibers in place. Several fibers are first positioned as the frame's warp (vertical fibers) at evenly spaced intervals. The weft fibers (horizontal fibers) are then interlaced with the warp using an 'over-under' pattern, reversing direction on each subsequent row to form a plain weave pattern. For the twill pattern, the weft fibers are woven in an 'over two, under one' sequence, with a one-fiber shift in each row to create a diagonal effect. A similar technique to the plain weave is applied in the basket weave pattern, but two weft and two warp fibers are woven together (two over, two under) to produce a checkerboard-like appearance. These steps are repeated until the weaving is complete, and the weave is tightened to ensure neatness and structural integrity. The weaving process is illustrated in Figure 5.

The advantage of plain weaving is its ease of fabrication, time efficiency, and strong weave. The plain weave structure was selected due to its tight construction and minimal yarn mobility, resulting in a sturdy and strong weave [32], [43], [44]. On the other hand, twill weaving offers good strength and durability due to its diagonal pattern, which evenly distributes the load and provides good drapability, as well as attractive visual aesthetics [45], [46], [47]. Meanwhile,

basket weaving involves two warp threads placed over two weft threads, with double interlocking at each crossing, which makes the load distribution more uniform, resulting in a structure that provides strength with slight flexibility, and enhances frictional force and strength per unit length during loading [48], [49]. Figure 5 below illustrates the water hyacinth fiber weaving pattern used in this study.

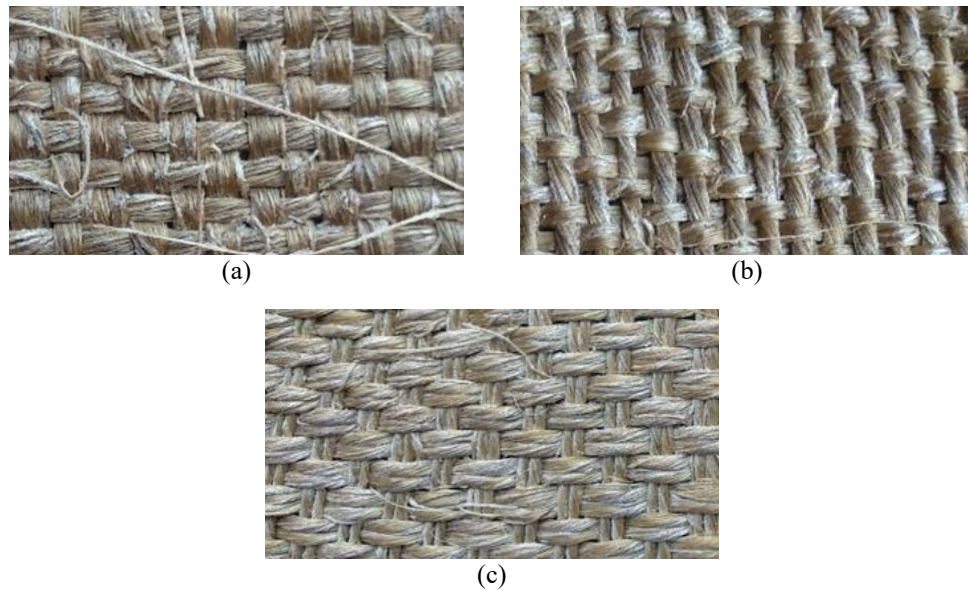


Figure 5. Water hyacinth fiber woven pattern (a) plain; (b) twill; (c) basket

2.4 Sample Fabrication

The alkali-treated water hyacinth fibers were twisted into 1.5 mm diameter ropes with 20 strands of fiber per twist, and then woven into sheets with plain, twill, and basket patterns, as shown in Figure 5. The next stage involves mixing epoxy resin and hardener in a 2:1 ratio in a measuring cup to create the matrix solution. The molding procedure involves the amalgamation of woven fiber sheets and epoxy resin within a mold of 150 mm × 200 mm × 50 mm, utilizing the hand lay-up technique. An adequate quantity of resin is introduced into the mold cavity. Subsequently, woven sheets are positioned in parallel on top of the resin. This process is repeated in layers, alternating between pouring resin and placing the woven sheets, until three layers of laminated composite are formed with parallel fiber orientation and a thickness of up to 6 mm. During the process, a roller is used to smooth the surface, ensure even resin distribution, and prevent air bubble formation [50]. This process further enhances the adhesion between the fabric and the matrix compared to conventional coating processes. The mold is, subsequently, allowed to cure at room temperature for 24 hours. Composite material is extracted from the mold for cutting after it has dried. Material waste is minimized by employing a hacksaw during the cutting procedure. The composite material must be cut in accordance with ISO 179 standards for impact testing and ASTM D790 standards for bending testing. To ensure precise and smooth edges that meet testing requirements, the specimen is to be sanded using sandpaper. Once the edges are soft, the specimen is cleaned with a cloth to remove dust. Figure 6 below shows the process flow in this study, from material preparation and fiber treatment to composite fabrication.

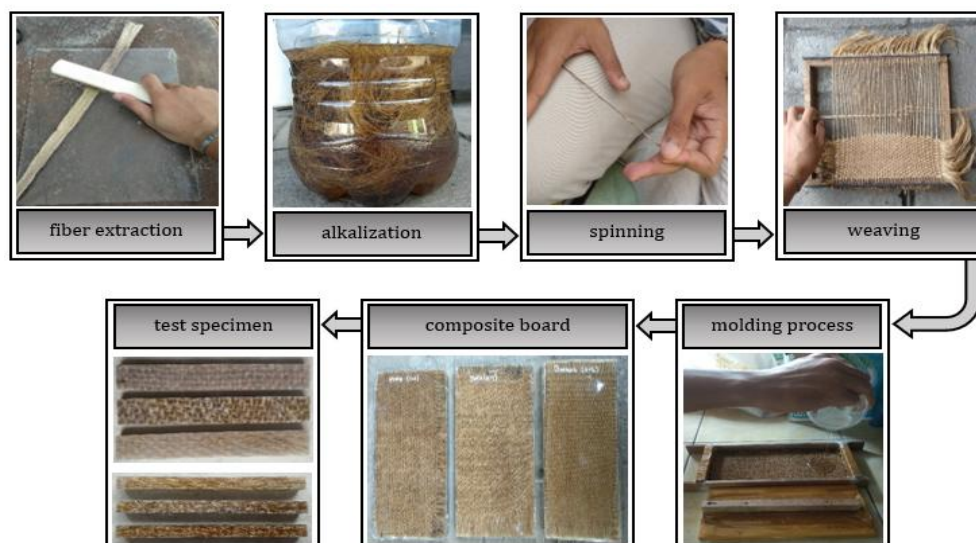


Figure 6. Composite manufacturing process

2.5 Impact Test

The research employs the Charpy impact test method according to ISO 179 standards, utilizing the GOTECH GT-7045-MD machine (Figure 7). The energy imparted to the specimen is 25 joules, accompanied by a pendulum velocity of 3.46 m/s. Before testing is conducted, the impact testing machine is calibrated to ensure accurate test results. The calibration is performed by operating the machine without a specimen to ensure that the initial and final energy values are zero, eliminating energy loss due to friction or reading errors. If discrepancies are found, the equipment will be adjusted or maintained. The impact test is conducted three times for each specimen variation, and the average value is calculated from the results.



Figure 7. (a) Impact testing machine; (b) Impact testing process

The impact test is performed to replicate the resilience of the test specimen under shock loads, to assess the material's mechanical characteristics and toughness value [31]. The results of this test indicate the amount of energy the material can absorb, allowing us to conclude whether the material is brittle or ductile. The absorbed energy from the test results is utilized to determine the impact intensity by employing the subsequent equation:

$$I_s = \frac{E}{A} \quad (1)$$

where I_s represents the impact intensity, E represents the impact energy, and A represents the area. Figure 8 illustrates the dimensions of the impact test specimen in accordance with the ISO 179 standard.

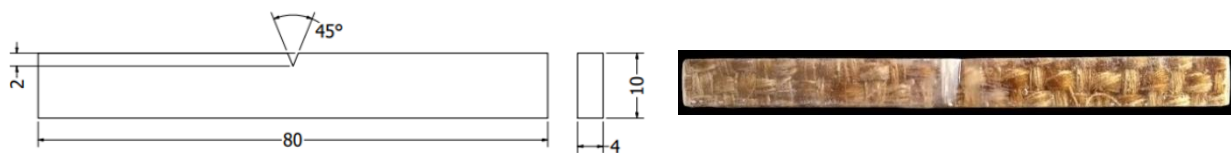


Figure 8. Impact test dimensions

2.6 Bending Test

The three-point bending method was followed under ASTM D-790 (Figure 9), and the testing was performed using a Gotech universal testing machine model UN-7001-LC30, series TC180200162 (2018). The testing apparatus was calibrated before the test to guarantee the reliability and accuracy of the bending test results. It is essential to verify the proper functioning of both the machine and the load measurement system, and to check the deflection indicators to ensure precision and consistency in the readings. Three tests were performed for each specimen variation in the bending test, and calculations were carried out to determine the average value.

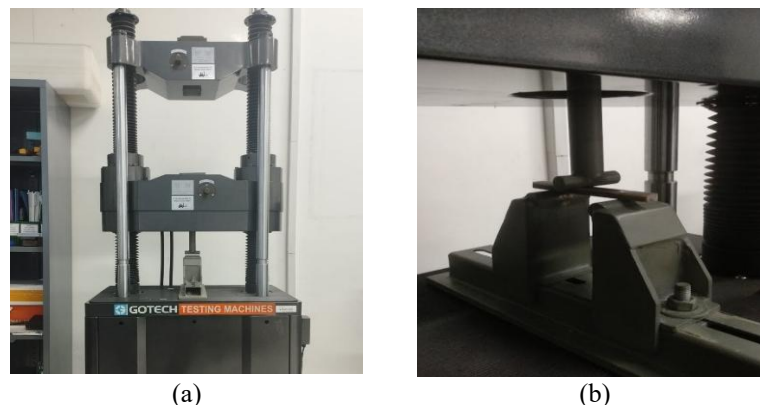


Figure 9. (a) Bending test machine; (b) Bending test process

During bending tests, the top section is subjected to compression. However, the lower section experiences tension, resulting in a fracture in the lower section that fails to endure the tensile stress. The bending test elucidates the behavior of materials when exposed to bending stresses under practical settings [51]. To calculate the modulus of elasticity and tensile strength using the equation:

$$\sigma = \frac{3FL}{2bd^2} \cdot E = \frac{FL^3}{4bd^3\delta} \tag{2}$$

where F is the greatest load that the test specimen can withstand, L, b, and d are the span length, breadth, and height, respectively, and δ is the energy that the specimen absorbs at the area where it is loaded. Figure 10 displays the size of the bending test specimen in accordance with ASTM D-790 standards.

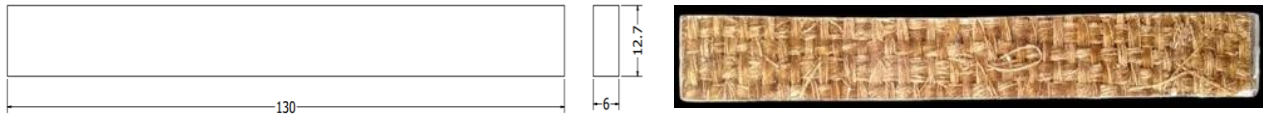


Figure 10. Bending test dimensions

3. RESULTS AND DISCUSSION

3.1 Fiber Surface Morphology

The microstructure analysis results, as illustrated in Figure 11, illustrate the surface diameter of a single water hyacinth fiber before and after alkali treatment. The fiber was observed through a microscope at a magnification of 50x. The diameter of the unadulterated water hyacinth fiber is 93.6423 μm, as illustrated in Figure 11(a). In contrast, Figure 11(b) illustrates the water hyacinth fiber that has been subjected to an alkali treatment with a 20% NaOH concentration for a duration of three hours. The diameter of the treated fiber is 54.4574 μm, which is 58.15% smaller than that of the untreated fiber.

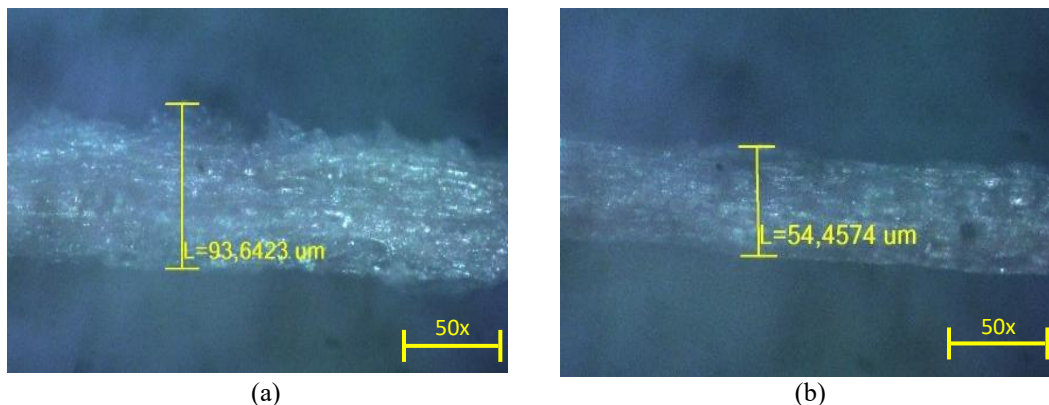


Figure 11. Fiber microphoto 50x magnification (a) before alkalization; (b) after alkalization

In this work, surface morphology photos of water hyacinth fibers reveal that soaking them in an alkaline solution can decrease their diameter. Fibers undergo shrinkage as a result of this treatment's elimination of lignin, hemicellulose, and other contaminants; at the same time, moisture content is reduced, which lessens the fibers' inherent hydrophilic characteristics while increasing the strength of the interfacial bond with the matrix [50], [52]. The fiber surface undergoes modification by alkaline treatment, as seen in Figure 3. This alteration can increase the adhesion to the polymer matrix, yielding composites with enhanced mechanical characteristics and greater environmental resilience. The mechanical strength and compatibility with the polymer composite matrix increase in fibers treated with NaOH [53].

3.2 Impact Test Result

From Figure 12, the impact test results on the specimens show that the water hyacinth fiber composite with a twill weave pattern has higher energy absorption and impact strength compared to other composite weave patterns, with values of 1.36 J and 0.034 J/mm², followed by the basket weave pattern with values of 1.23 J and 0.031 J/mm². In contrast, the plain weave pattern showed the lowest values, namely 0.9 J and 0.023 J/mm². For comparison, the energy absorption and impact strength values for the car bumper specimen were recorded at 1.07 J and 0.027 J/mm², which are lower than those of the twill and basket patterns but higher than those of the plain pattern.

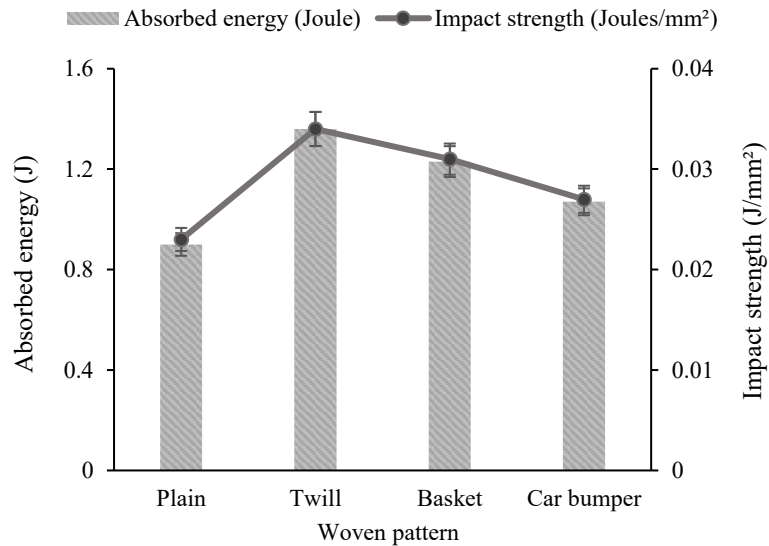


Figure 12. Effect of impact properties on different weave patterns

Based on the impact strength of the composite woven patterns above, the composite with the twill woven pattern exhibits the highest impact strength. In contrast, the composite with the plain-woven pattern shows the lowest impact strength. This is because the twill woven pattern provides good strength and durability to the weave, as it has more crossings and a higher angle of yarn compared to the plain-woven pattern, allowing the shock load applied to the composite to be well distributed across the weave, resulting in strong interlocking [54]. The high crimp of the yarn in the twill pattern compared to other woven patterns also significantly reduces damage from impacts and increases the laminate's damage tolerance [55], [56]. The vertical and horizontal crossings are critical in determining the strength of the weave, as the number of crossings, interlocking, and the structure of the woven pattern affect the distribution of composite strength in an evenly distributed manner, withstanding loads [57]. Twill weave is typically more flexible than other patterns, such as plain weave, which enables it to absorb impact energy more effectively. Its distinctive diagonal fiber arrangement also contributes to greater tensile strength and improved resistance to deformation, resulting in better overall structural performance [58]. This structural advantage comes from the intersecting fiber directions, which enhance the material's ability to withstand impact and minimize damage.

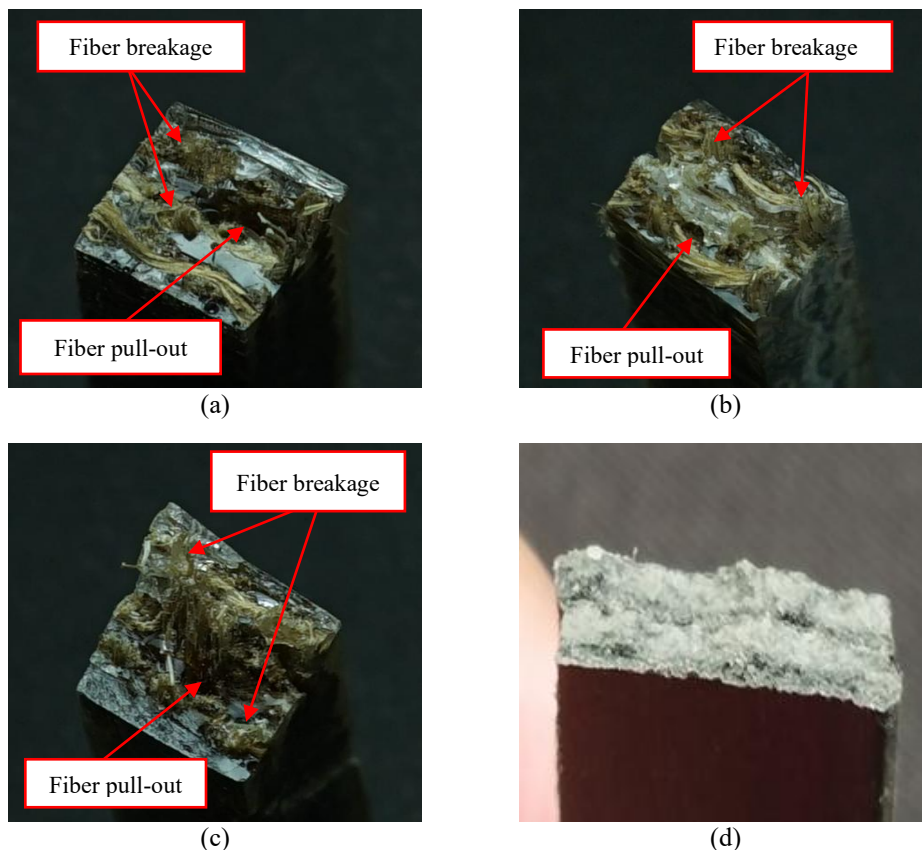


Figure 13. Fracture of impact test specimen (a) plain; (b) twill; (c) basket; (d) car bumper

The fracture analysis results on the impact test specimens are illustrated in Figure 13, which illustrates the occurrence of fiber pull-out. Although the fibers were alkalized, this condition was observed in all test specimens due to the insufficient adhesion between the fiber and the matrix [50]. Fiber pull-out occurs when the interfacial link between the fiber and the matrix is inadequately robust to maintain cohesion under impact loading [59]. The insufficient resin penetration into the inter-fiber cavities and the lack of chemical compatibility between the hydrophilic fiber surface and the hydrophobic polymer matrix are the possible causes of this feeble adhesion [60]. These conditions may act as stress concentration points or crack initiation sites when impact loading is applied, reducing energy absorption capacity. In addition, fiber breakage was also observed in the natural fiber composites, which occurs when the fibers are damaged and fracture under mechanical loads exceeding their tensile strength. Fiber breakage indicates that the load was effectively transferred from the matrix to the fiber until it reached its ultimate strength. Therefore, fiber breakage reflects relatively better interfacial stress transfer than fiber pull-out failure [61]. Despite the presence of both fiber pull-out and fiber breakage, the vertical and horizontal interlacing points in the plain weave pattern help distribute the load more evenly and enhance the material's ability to absorb impact energy to the maximum extent, owing to the mechanical interlocking effect that reinforces the composite structure.

3.3 Bending Test Result

Based on the average bending strength graph in Figure 14, this study shows that the twill weave pattern has the highest bending strength compared to other composite weave patterns, with a value of 122.9 MPa. Next, the basket weave pattern has a value of 90.7 MPa, while the composite with a plain weave pattern shows a value of 51.7 MPa. This value is lower than the bending strength of the car bumper specimens, which is 86.2 MPa. The results of the bending strength show that the twill woven pattern yields the highest bending strength, while the plain-woven composite pattern results in the lowest bending strength. This results from the attributes of the woven construction of the twill pattern. This design features bigger interstices than other woven patterns, hence improving the mechanical adhesion between the fibers and the matrix [62]. Complex weaving patterns, such as the twill weave, distribute damage more uniformly. This behavior is attributed to the enhanced ability of the fibers within these patterns to conform to applied loads, thereby minimizing stress concentration and reducing localized damage [57].

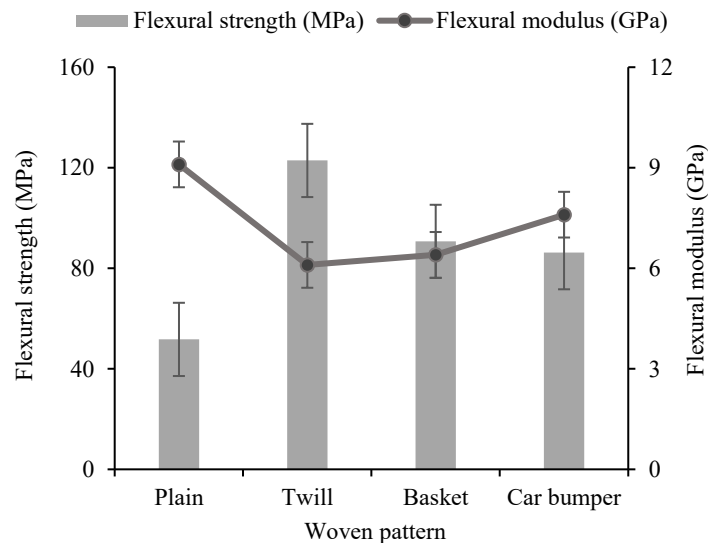


Figure 14. Effect of flexural strength and flexural modulus on different weave patterns

Another factor influencing the twill woven pattern's strength is the threads' cross-direction. In twill weaving, the points of intersection between the threads run diagonally, forming a diagonal line pattern. This diagonal pattern plays a role in distributing the load evenly, making the weave more resistant to strain and pressure [63], [64]. This ultimately contributes to enhanced structural performance. Although the twill weave exhibits the highest impact resistance, its superior structural performance is attributed not only to its impact resistance but also to the inherent characteristics of its diagonal pattern, which facilitates a more effective distribution of forces and improves the material's overall strength [65]. Additionally, the twill woven pattern also has good drapability.

Meanwhile, in terms of elastic modulus, the plain weave pattern exhibited the highest value at 9.1 GPa, followed by the car bumper at 7.6 GPa, the basket weave pattern at 6.4 GPa, and the lowest was the twill weave pattern at 6.1 GPa. Based on the analysis in Figure 14, it can be concluded that the elastic modulus is inversely proportional to the flexural strength. These results align with the research undertaken by Wu et al. [66] and Tefera et al. [67], which indicate that composite materials with high flexural strength tend to have lower flexural modulus values. This suggests that materials with high flexural strength can withstand greater loads before breaking, but are more flexible due to their lower modulus. The flexural modulus is a measure of the material's rigidity during the elastic phase of loading, while flexural strength is a measure of its resistance to failure under continuous loading. The bond strength between the fibers and the matrix

influences flexural strength, while the weave pattern structure and fiber orientation have a greater impact on flexural modulus. In this instance, the material is capable of withstanding substantial bending stresses before failing, while also remaining sufficiently flexible, allowing it to undergo significant deformation before reaching its breaking point [68] [69].

Several phenomena were disclosed by the flexural test results on fractured specimens, as illustrated in Figure 15. The fibers were hauled out due to the low adhesion between the fibers and the matrix, even though the fibers had undergone alkali treatment. This was due to the decreasing binding between the epoxy resin and the fibers as the load increased. Interfacial adhesion has a substantial impact on the mechanical efficacy of fiber-reinforced composites. The robust interfacial bonding that occurs during the stress transfer process between the matrix and the fibers enables the composite to withstand loads that exceed its strain limits [70]. However, powerful interfacial bonds can initiate crack propagation, ultimately reducing the toughness and strength of the material [71]. Moreover, fiber breakage was noted, resulting in the fracturing of natural fibers inside the composite, which further impacted its mechanical capabilities [72]. All samples exhibited a typical failure mechanism characterized by a combination of fiber pull-out and fiber breakage, with the extent of damage varying according to the arrangement of the woven structure. Nevertheless, the composite with a twill weave pattern exhibited a lower level of fiber damage as a result of the diagonal alignment of the strands. This alignment facilitates the more even distribution of the load, delays the initiation of cracks, and enhances resistance to flexural loads compared to other weave pattern configurations. As a result, the interfacial bonding quality and weave configuration have a substantial impact on the composite's mechanical performance and durability.

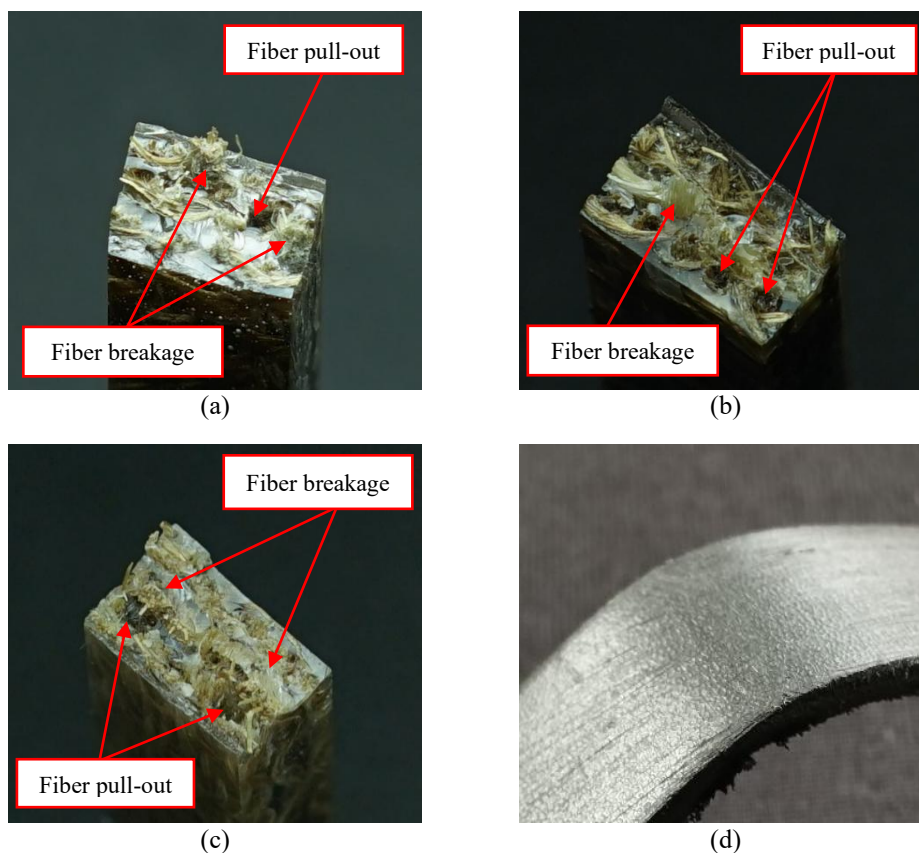


Figure 15. Fracture of bending test specimen (a) plain; (b) twill; (c) basket; (d) car bumper

4. CONCLUSIONS

The utilization of water hyacinth fiber as reinforcement in composites aims to provide an alternative material to non-renewable resources, especially within the automotive sector. This research investigates the influence of various weaving patterns on the mechanical strength of the material. Testing results indicate that the twill weave pattern provides the highest impact and bending strength values, at 0.034 J/mm^2 and 122.9 MPa , respectively, compared to other weave patterns. Furthermore, cross-sectional examination of specimen fractures resulting from bending and impact testing reveals prevalent failures, including fiber pull-out and breaking. Nonetheless, a reduced degree of fiber damage in the twill weave composite enhances its load-bearing capacity compared to other weave configurations, hence influencing the composite's bending and impact strength. Additionally, the mechanical strength analysis of the water hyacinth fiber composite with twill and basket weaves yielded higher values than the car bumper specimen used as a product control. Therefore, the findings from this study suggest that water hyacinth fiber has excellent potential to produce competitive and environmentally friendly materials for automotive applications, particularly as an alternative to traditional materials for car bumpers. Moreover, utilizing water hyacinth plants as natural fiber composite materials is expected to provide a

solution for managing this plant, which is considered a weed in various aquatic areas worldwide. As such, it can contribute to the Sustainable Development Goals (SDGs) through advancing resource efficiency and environmental sustainability.

ACKNOWLEDGEMENTS

The author would like to thank the Department of Mechanical Engineering, Faculty of Engineering, Universitas Negeri Semarang (UNNES) for providing laboratory facilities and its support.

CONFLICT OF INTEREST

The authors declare no conflicts of interest

AUTHORS CONTRIBUTION

Muhammad Arryanto (Writing - Original Draft; Conceptualisation; Investigation; Resources; Supervision)

Heri Yudiono (Validation; Formal analysis; Supervision)

Januar Parlaungan Siregar (Writing - review & editing; Formal analysis)

Tezara Cionita (Writing - review & editing; Formal analysis)

Deni Fajar Fitriyana (Writing - review & editing; Formal analysis)

Al Ichlas Imran (Writing - review & editing; Formal analysis)

REFERENCES

- [1] N. Athirah, N. Mahdi, Y. Fernando, and A. Ibrahim, "Revealing the path to a green economy: Insights and recommendations for sustainable development in Malaysia," *International Journal of Integrated Engineering*, vol. 16, no. 2, pp. 245–258, 2024.
- [2] T. Cionita, J. Jaafar, J. P. Siregar, S. M. A. S. A. Karim, M. F. Zulkiflee, M. I. Shamsuddin, et al., "Mechanical characteristics of biocomposites based on rice husk reinforced recycled polypropylene," *International Journal of Integrated Engineering*, vol. 16, no. 2, pp. 278–287, 2024.
- [3] B. T. Mulyo and H. Yudiono, "Toughness analysis of pineapple leaves fiber composite as alternative material for SNI helmet," *Journal of Mechanical Engineering and Sciences*, vol. 13, no. 4, pp. 5961–5972, 2019.
- [4] K. Sukiyono, M. M. Romdhon, G. Mulyasari, M. Z. Yuliarso, T. Agung, D. M. T. Napitupulu, et al., "Smallholder palm oil and sustainable development goals (SDGs) achievement: An empirical analysis," *Sustainable Futures*, vol. 8, pp. 1–15, 2024.
- [5] M. R. Sanjay, S. Siengchin, J. Parameswaranpillai, M. Jawaid, C. I. Pruncu, and A. Khan, "A comprehensive review of techniques for natural fibers as reinforcement in composites: Preparation, processing and characterization," *Carbohydrate Polymers*, vol. 207, pp. 108–121, 2019.
- [6] M. S. Bisht, M. Singh, A. Chakraborty, and V. K. Sharma, "Genome of the most noxious weed water hyacinth (*Eichhornia crassipes*) provides insights into plant invasiveness and its translational potential," *iScience*, vol. 27, no. 9, pp. 1–19, p. 110698, 2024.
- [7] R. D. Ratnani, F. D. Arianti, and N. A. Sasongko, "Exploring the potential of water hyacinth weed (*Pontederia crassipes*) as an environmentally friendly antifungal to realize sustainable development in lakes: A review," *Case Studies in Chemical and Environmental Engineering*, vol. 9, pp. 1–8, 2024.
- [8] M. A. Bote, V. R. Naik, and K. B. Jagadeeshgouda, "Review on water hyacinth weed as a potential bio fuel crop to meet collective energy needs," *Materials Science for Energy Technologies*, vol. 3, pp. 397–406, 2020.
- [9] Y. A. Damtie, D. A. Mengistu, and D. T. Meshesha, "Spatial coverage of water hyacinth (*Eichhornia crassipes* (Mart.) Solms) on Lake Tana and associated water loss," *Heliyon*, vol. 7, no. 10, pp. 1–8, 2021.
- [10] R. Dhinesh, S. Aruna, K. Ravaneswaran, S. S. Kirthiga, S. G. Keerthivarman, K. A. Al-Ghanim, et al., "Aquatic weed *Eichhornia crassipes* as sustainable feedstocks for biochar production: A potential of ammonium adsorption and kinetic models," *Journal of Cleaner Production*, vol. 459, pp. 1–14, 2024.
- [11] M. M. Owen, E. O. Achukwu, and H. Md Akil, "Preparation and mechanical characterizations of water hyacinth fiber based thermoset epoxy composite," *Journal of Natural Fibers*, vol. 19, no. 16, pp. 13970–13984, 2022.
- [12] K. Jia, Q. Sheng, Y. Liu, Y. Yang, G. Dong, Z. Qiao, et al., "A framework for achieving urban sustainable development goals (SDGs): Evaluation and interaction," *Sustainable Cities and Society*, vol. 114, pp. 1–12, 2024.
- [13] M. A. Basith, N. C. Reddy, S. Uppalapati, and S. P. Jani, "Crash analysis of a passenger car bumper assembly to improve design for impact test," in *Materials Today: Proceedings*, Elsevier Ltd, 2021, pp. 1684–1690.
- [14] V. A. Sumahi, S. P. Jani, and S. Uppalapati, "Impact study of a car bumper by using carbon fiber reinforced polyetherimid and S-glass/ epoxy composite," *Materials Today: Proceedings*, vol. 92, pp. 364–370, 2023.
- [15] M. S. Ul Abrar, K. F. Nadim Ezaz, M. J. Hasan, R. I. Pranto, T. A. Alvy, and M. Z. Hossain, "Speed-dependent impact analysis on a car bumper structure using various materials," *Results in Engineering*, vol. 21, pp. 1–11, 2024.
- [16] A. A. G. Olorunnishola and E. G. Adubi, "A comparative analysis of a blend of natural jute and glass fibers with synthetic glass fibers composites as car bumper materials," *IOSR Journal of Mechanical and Civil Engineering*, vol. 15, no. 3, pp. 67–71, 2018.

- [17] S. Boria, C. Santulli, E. Raponi, F. Sarasini, and J. Tirillò, "Analytical modeling and experimental validation of the low-velocity impact response of hemp and hemp/glass thermoset composites," *Journal of Composite Materials*, vol. 54, no. 3, pp. 409-421, 2020.
- [18] A. Gholampour and T. Ozbakkaloglu, "A review of natural fiber composites: Properties, modification and processing techniques, characterization, applications," *The Journal of Materials Science*, vol. 55, no. 3, pp. 829-892, 2020.
- [19] N. Nawawithan, P. Kittisakpairach, S. Nithiboonyapun, K. Ruangjirakit, and P. Jongpradist, "Design and performance simulation of hybrid hemp/glass fiber composites for automotive front bumper beams," *Composite Structures*, vol. 335, pp. 1-10, 2024.
- [20] W. Su, Q. Sun, M. Xia, Z. Wen, and Z. Yao, "The resource utilization of water hyacinth (*Eichhornia crassipes* [Mart.] Solms) and its challenges," *Resources*, vol. 7, no. 46, pp. 1-9, 2018.
- [21] J. Darmanto, "The effect of fiber pretreatment on physical and mechanical properties in water hyacinth fiber composite," *International Journal of Emerging Trends in Engineering Research*, vol. 8, no. 8, pp. 4799-4805, 2020.
- [22] V. Keryvin, P. Y. Méchin, E. Fabing, I. Pillin, K. Mahé-Flahaut, and A. Le Palabe, "Counter-intuitive effect of the degree of cure of epoxy resins on the compressive strength of continuous fibre composites," *Composites Part B: Engineering*, vol. 287, pp. 1-6, 2024.
- [23] A. Dass and S. Chellamuthu, "Physico chemical and mechanical properties of natural cellulosic water hyacinth fiber and its composites," *Journal of Natural Fibers*, vol. 19, no. 15, pp. 11413-11423, 2022.
- [24] J. Yang, K. Zhang, D. Chen, Y. Zhang, X. Zhang, and Z. Yang, "Effect of alkali treatment on water absorption deterioration and mechanism of wheat straw/PVC composites," *Polymer Testing*, vol. 131, pp. 1-12, 2024.
- [25] R. Paul, K. Gouda, and S. Bhowmik, "Effect of different constraint on tribological behaviour of natural fibre/filler reinforced polymeric composites: A review," *Silicon*, vol. 13, no. 8, pp. 2785-2807, 2021.
- [26] Kusmono, H. Hestiawan, and Jamasri, "The water absorption, mechanical and thermal properties of chemically treated woven fan palm reinforced polyester composites," *Journal of Materials Research and Technology*, vol. 9, no. 3, pp. 4410-4420, 2020.
- [27] N. S. Nor Arman, R. S. Chen, and S. Ahmad, "Review of state-of-the-art studies on the water absorption capacity of agricultural fiber-reinforced polymer composites for sustainable construction," *Construction and Building Materials*, vol. 302, pp. 1-14, 2021.
- [28] P. Valášek, M. Müller, V. Šleger, V. Kolář, M. Hromasová, R. D'Amato, et al., "Influence of alkali treatment on the microstructure and mechanical properties of coir and abaca fibers," *Materials*, vol. 14, no. 10, pp. 1-20, 2021.
- [29] R. Belliveau, B. Landry, and G. LaPlante, "Comparative study of the mechanical properties of woven and unidirectional fibres in discontinuous long-fibre composites," *Journal of Thermoplastic Composite Materials*, vol. 36, no. 6, pp. 2372-2389, 2023.
- [30] F. Yudhanto, A. Wisnujati, V. Yudha, P. Rachmawati, and K. R. Dantes, "Effect of chemical treatments on morphological, physical and mechanical properties of bamboo/ glass fibers hybrid laminated composite," *International Journal of Integrated Engineering*, vol. 13, no. 7, pp. 315-323, 2021.
- [31] H.- Yudiono and M.T.N. Fuad, "The effect of Aegle marmelos shell particles volume fraction on hardness, toughness, and wear rate of epoxy matrix composites as motorcycle brake pads," *Journal of Mechanical Engineering and Sciences*, vol. 17, pp. 9338-9348, 2023.
- [32] M. Y. Yaakob, M. A. Husin, A. Abdullah, K. A. Mohamed, A. S. Khim, M. L. C. Fang, et al., "Effect of stitching patterns on tensile strength of kenaf woven fabric composites," *International Journal of Integrated Engineering*, vol. 11, no. 6, pp. 70-79, 2019.
- [33] S. Prasetyo, S. Anggoro, and T. R. Soeprbowati, "The growth rate of water hyacinth (*Eichhornia Crassipes* (Mart.) Solms) in Rawapening Lake, Central Java," *Journal of Ecological Engineering*, vol. 22, no. 6, pp. 222-231, 2021.
- [34] A. Nugroho, D. M. Maharani, A. C. Legowo, S. Hadi, and F. Purba, "Enhanced mechanical and physical properties of starch foam from the combination of water hyacinth fiber (*Eichhornia crassipes*) and polyvinyl alcohol," *Industrial Crops and Products*, vol. 183, pp. 1-8, 2022.
- [35] B. D. Wembe, N. C. Wiriyikfu, G. E. Ntamack, B. Kenmeugne, T. Tchotang, D. Rolland, et al., "Extraction and physicochemical and thermomechanical characterizations of water hyacinth fibers *eichhornia crassipes*," *International Journal of Polymer Science*, vol. 2023, pp. 1-9, 2023.
- [36] A. Bin Rashid, A. M. Rayhan, S. I. Shaily, and S. M. M. Islam, "An experimental study of physical, mechanical, and thermal properties of Rattan fiber reinforced hybrid epoxy resin laminated composite," *Results in Engineering*, vol. 22, pp. 1-11, 2024.
- [37] I. D. S. Silva, J. J. P. Barros, A. Albuquerque, N. G. Jaques, M. V. L. Fook, and R. M. R. Wellen, "Insights into the curing kinetics of EPOXY/PLA: Implications of the networking structure," *Express Polymer Letters*, vol. 14, no. 12, pp. 1180-1196, 2020.
- [38] C. Verma, L. O. Olasunkanmi, E. D. Akpan, M. A. Quraishi, O. Dagdag, M. El Gouri, et al., "Epoxy resins as anticorrosive polymeric materials: A review," *Reactive and Functional Polymers*, vol. 156, pp. 1-20, 2020.
- [39] S. Alemyayehu, Y. Regassa, B. Yoseph, and H. G. Lemu, "Mechanical Properties Characterization of Water Hyacinth ('Emboch') Plant for Use as Fiber Reinforced Polymer Composite," in *Lecture Notes of the Institute for Computer Sciences, Social-Informatics and Telecommunications Engineering, LNICST*, Springer Science and Business Media Deutschland GmbH, 2021, pp. 482-492.
- [40] R. S. N. Sahai and R. A. Pardeshi, "Comparative study of effect of different coupling agent on mechanical properties and water absorption on wheat straw-reinforced polystyrene composites," *Journal of Thermoplastic Composite Materials*, vol. 34, no. 4, pp. 433-450, 2021.

- [41] C. I. Madueke, S. D. Pandita, F. Biddlestone, and G. F. Fernando, "Effects of NaOH treatment and NaOH treatment conditions on the mechanical properties of coir fibres for use in composites manufacture," *Journal of the Indian Academy of Wood Science*, vol. 21, no. 1, pp. 100–111, 2024.
- [42] S. Arumugam, J. Kandasamy, S. Venkatesan, R. Murugan, V. L. Narayanan, M. T. Sultan, et al., "A review on the effect of fabric reinforcement on strength enhancement of natural fiber composites," *Materials*, vol. 15, no. 9, pp. 1-33, 2022.
- [43] S. Jeyaguru, S. M. K. Thiagamani, S. Siengchin, J. Subramanian, H. Ebrahimnezhad-Khaljiri, M. R. Sanjay, et al., "Effect of various weaving architectures on mechanical, vibration and acoustic behavior of Kevlar-Hemp intra-ply hybrid composites," *Composites Part A: Applied Science and Manufacturing*, vol. 176, pp. 1-13, 2024.
- [44] K. Rassiah, A. Ali, and M. Saeman, "Evaluation the effect of laminated layer sequence of plain-woven bamboo on tensile and impact performance of e-glass woven/ epoxy hybrid composites," *International Journal of Integrated Engineering*, vol. 13, no. 5, pp. 194–200, 2021.
- [45] Z. X. Lei, J. Ma, W. K. Sun, B. B. Yin, and K. M. Liew, "Low-velocity impact and compression-after-impact behaviors of twill woven carbon fiber/glass fiber hybrid composite laminates with flame retardant epoxy resin," *Composite Structures*, vol. 321, pp. 1-14, 2023.
- [46] S. N. A. Khalid, M. H. Zainulabidin, A. M. T. Arifin, M. F. Hassasn, M. R. Ibrahim, and M. Z. Rahim "Mechanical performances of twill kenaf woven fiber reinforced polyester composites," *International Journal of Integrated Engineering*, vol. 10, no. 4, pp. 49–59, 2018.
- [47] J. Lee, W. Kim, J. Kim, M. Um, S. W. Kim, J. W. Yi, et al., "A two-layered cross-ply laminate model for a single-ply satin woven fabric composite under thermal loads," *Composite Structures*, vol. 351, p. 118619, pp. 1-14, 2025.
- [48] H. Wu, X. Li, K. Yan, M. Yuan, C. Huang, and Q. Zhang, "Influence of weft yarn distribution on 3D woven composites under impact loading," *International Journal of Mechanical Sciences*, vol. 284, pp. 1-55, p. 109762, 2024.
- [49] S. Jeyaguru, S. M. K. Thiagamani, H. Pulikkalparambil, S. Siengchin, J. Subramaniam, S. M. Rangappa, et al., "Mechanical, acoustic and vibration performance of intra-ply Kevlar/PALF epoxy hybrid composites: Effects of different weaving patterns," *Polymer Composites*, vol. 43, no. 6, pp. 3902–3914, 2022.
- [50] C. Tezara, M. Zalinawati, J. P. Siregar, J. Jaafar, M. H. M. Hamdan, A. N. Oumer, et al., "Effect of stacking sequences, fabric orientations, and chemical treatment on the mechanical properties of hybrid woven jute-ramie composites," *International Journal of Precision Engineering and Manufacturing - Green Technology*, vol. 9, no. 1, pp. 273–285, 2022.
- [51] N. L. Feng, S. D. Malingam, and C. W. Ping, "Mechanical characterisation of kenaf/PALF reinforced composite-metal laminates: Effects of hybridisation and weaving architectures," *Journal of Reinforced Plastics and Composites*, vol. 40, no. 5–6, pp. 193–205, 2021.
- [52] A. Arivendan, W. J. Jebas Thangiah, A. Mahaboob Basha, B. Chris, and J. Haider, "Studying mechanical, thermal and absorption, characteristics of water hyacinth (eichhornia crassipes) plant fibre reinforced polymer composites," *Journal of Natural Fibers*, vol. 19, no. 16, pp. 13958–13969, 2022.
- [53] P. Lokesh, T. S. A. Surya Kumari, R. Gopi, and G. B. Loganathan, "A study on mechanical properties of bamboo fiber reinforced polymer composite," in *Materials Today: Proceedings*, Elsevier Ltd, 2020, pp. 897–903.
- [54] H. Tewani, J. Cyvas, K. Perez, and P. Prabhakar, "Ar χ i-Textile composites: Role of weave architecture on mode-I fracture energy in woven composites," *Composites Part A: Applied Science and Manufacturing*, vol. 188, pp. 1-11, p. 108499, 2025.
- [55] H. Dalfi, K. B. Katnam, and P. Potluri, "Intra-laminar toughening mechanisms to enhance impact damage tolerance of 2D woven composite laminates via yarn-level fiber hybridization and fiber architecture," *Polymer Composites*, vol. 40, no. 12, pp. 4573–4587, 2019.
- [56] A. Dixit, R. K. Misra, and H. S. Mali, "Finite Element Compression Modelling of 2x2 Twill Woven Fabric Textile Composite," *Procedia Materials Science*, vol. 6, pp. 1143–1149, 2014.
- [57] F. Liu, L. Grotz, Y. Cui, and K. Kirane, "Experimental dataset on the in-plane tensile, shear, and compressive properties of a carbon-epoxy twill woven composite," *Data Brief*, vol. 45, pp. 1-24, 2022.
- [58] N. D. Raja, K. V. Anand Kumar, S. Salunkhe, and H. M. A. Hussein, "Investigation of water absorption properties of 2D interwoven kevlar-jute reinforced hybrid laminates," *Journal of Composites Science*, vol. 7, no. 5, pp. 1-14, 2023.
- [59] H. Yudiono, J. P. Siregar, S. Asri, H. Hidayat, D. B. Chikam, J. A. Aprilian, et al., "Effect of alkalization time on the toughness and strength of jute sack waste lamina composite as an alternative car bumper material," *International Journal of Automotive and Mechanical Engineering*, vol. 21, no. 4, pp. 11809–11820, 2024.
- [60] C. H. Lee, A. Khalina, and S. H. Lee, "Importance of interfacial adhesion condition on characterization of plant-fiber-reinforced polymer composites: A review," *Polymers*, vol. 13, pp. 1-22, 2021.
- [61] P. K. Rakesh, J. Kumar, V. Kumar, and I. Singh, "Joining behavior of bio-filler-based polyester composites," in *Polylactic Acid Composites: Sustainable Biocomposites*, De Gruyter, 2023, pp. 257–269.
- [62] K. B. Katnam, H. Dalfi, and P. Potluri, "Towards balancing in-plane mechanical properties and impact damage tolerance of composite laminates using quasi-UD woven fabrics with hybrid warp yarns," *Composite Structures*, vol. 225, pp. 1-13, 2019.
- [63] C. Anand Chairman, S. Jayasathyakawin, S. P. Kumaresh Babu, and M. Ravichandran, "Mechanical properties of basalt fabric plain and twill weave reinforced epoxy composites," in *Materials Today: Proceedings*, Elsevier Ltd, 2019, pp. 9480–9483.
- [64] P. Sharma, P. Priyanka, H. S. Mali, and A. Dixit, "Geometric modeling and finite element analysis of kevlar monolithic and carbon-kevlar hybrid woven fabric unit cell," in *Materials Today: Proceedings*, Elsevier Ltd, 2019, pp. 766–774.
- [65] G. M. Kanaginahal, H. S. Hebbar, and S. M. Kulkarni, "Influence of weave pattern and composite thickness on mechanical properties of bamboo/epoxy composites," *Materials Research Express*, vol. 6, no. 12, pp. 1-12, 2019.

- [66] M. S. Wu, B. C. Jin, X. Li, and S. Nutt, "A recyclable epoxy for composite wind turbine blades," *Advanced Manufacturing: Polymer and Composites Science*, vol. 5, no. 3, pp. 114–127, 2019.
- [67] G. Tefera, G. Bright, and S. Adali, "Flexural and shear properties of CFRP laminates reinforced with functionalized multiwalled CNTs," *Nanocomposites*, vol. 7, no. 1, pp. 141–153, 2021.
- [68] P. RaviKumar, G. Rajeshkumar, J. Prakash Maran, N. A. Al-Dhabi, and P. Karuppiyah, "Evaluation of mechanical and water absorption behaviors of jute/carbon fiber reinforced polyester hybrid composites," *Journal of Natural Fibers*, vol. 19, no. 13, pp. 6521–6533, 2022.
- [69] M. M. H. Parvez, S. M. Nur Rupom, M. M. Adil, T. Tasnim, M. S. Rabbi, and I. Ahmed, "Investigation of mechanical properties of rattan and bamboo fiber reinforced vinyl ester composite material for automotive application," *Results in Materials*, vol. 19, pp. 1-8, 2023.
- [70] F. S. da Luz, F. da Costa Garcia Filho, M. T. G. del-Río, L. F. Cassiano Nascimento, W. A. Pinheiro, and S. N. Monteiro, "Graphene-incorporated natural fiber polymer composites: A first overview," *Polymers*, vol. 12, pp. 1-36, 2020.
- [71] S. O. Amiandamhen, M. Meincken, and L. Tyhoda, "Natural Fibre Modification and Its Influence on Fibre-matrix Interfacial Properties in Biocomposite Materials," *Fibers and Polymers*, vol. 21, no. 4, pp. 677-689, 2020.
- [72] Z. Khan, B. F. Yousif, and M. Islam, "Fracture behaviour of bamboo fiber reinforced epoxy composites," *Composites Part B: Engineering*, vol. 116, pp. 186–199, 2017.